

Motion-compensated temporal summation of cardiac gated SPECT images using a deformable mesh model

Thibault Marin, *Student Member, IEEE* Miles N. Wernick, *Senior Member, IEEE*, Yongyi Yang, *Senior Member, IEEE* and Jovan G. Brankov, *Senior Member, IEEE*
Illinois Institute of Technology, ECE Dept., Medical Imaging Research Center

Abstract— We propose a motion-compensated non-rigid summation method for noise reduction in cardiac gated SPECT. This approach generates a static SPECT image containing counts from all frames of the gated sequence while accounting for heart motion to avoid motion-blur artifact. Static cardiac images typically suffer from heart motion occurring during acquisition which introduces the so-called motion blur artifact. Gated acquisitions, on the other hand, are characterized by lower counts in each individual frame, thus resulting in noisy images. Methods have been proposed to sum the gated sequence along the time dimension while accounting for heart motion, but they do not account for partial volume effect, manifested by an intensity increase as the myocardium contracts. The partial volume effect, a useful diagnostic feature has to be accounted for during both motion estimation and temporal summation. The proposed method relies on a deformable mesh model to estimate heart motion while accounting for the partial volume effect. The estimated motion is further used to perform non-rigid summation along the time dimension. We show that the proposed method yields visual improvement on clinical data. In addition, quantitative evaluation from phantom studies proves that the proposed method achieves better noise reduction performance than available clinical techniques.

I. INTRODUCTION

Single photon emission computed tomography (SPECT) is often used for cardiac imaging in order to assess myocardial function. Cardiac SPECT typically allows for detection of perfusion defects or abnormality in heart motion (via left ventricular ejection fraction measurements [1] or ventricular strain [2]). Several clinical protocols are available, such as static and gated acquisitions. The first method collects emitted photons during the whole acquisition yielding a unique time frame, while the latter divides acquisition into multiple time frames over one heart cycle. Gated imaging results in lower counts in each time frame compared to static acquisition, thus resulting in more severe noise in projection images. However, since the heart is experiencing motion during acquisition, static modalities introduce the so called motion blur artifact, which degrades image quality. Nevertheless, static images are often preferred in a clinical environment since their visualization requires a simpler setup than visualization of a gated sequence. In [3], a technique has been proposed to perform non-rigid summation of gated sequences to yield a static frame while

correcting for motion blur artifact. This method relies on grid deformation using heart motion estimated via optical flow [4]. More recently, a similar summation technique was proposed in [5], [6] where motion estimation is performed by detecting the left ventricle surfaces (endocardial and epicardial), and assuming that heart motion is normal to these surfaces. This approach improves diagnostic accuracy for detection of coronary artery disease. However the method used in [3] does not account for partial volume effect (PVE) [7], which appears as the heart wall contracts and is a diagnostic feature used to assess wall motion. Additionally, the motion estimation procedure introduced in [5] considers only motion orthogonal to the endocardial and epicardial surfaces. The proposed method uses a motion estimation technique, published in [8]–[10], which accounts for partial volume effect and which does not have any prior assumption on the heart motion.

The proposed algorithm relies on a mesh representation of the left ventricle, initialized using the left ventricle model reported in [11], and tracking heart motion as described in [8]. The estimated motion is then used to perform motion-compensated summation along the time dimension. The previously published work [8]–[10] applies 4D filtering on reconstructed images thus yielding a temporal sequence while the proposed method generates a single static image containing counts from all frames. This paper offers a quantitative evaluation of the proposed algorithm by incorporating noise reduction assessment based on multiple noise realizations. Other approaches can be considered for motion compensation of gated SPECT images. Post reconstruction filters have been reported [12], [13] where temporal information is used to perform accurate filtering. In addition, several methods have been introduced to integrate heart motion in image reconstruction, such as [14]–[16]. These methods result in gated sequences, while the proposed method aims at correcting blur artifacts in static images. In this paper, we first introduce the mesh model used for motion estimation and nonrigid summation along the time dimension. Further, we discuss the quantitative results obtained when applying the proposed method.

II. METHODS

In this section, we describe the deformable mesh model used to, first track the heart motion, and further perform motion-compensated summation along time dimension.

This work was supported by the National Institutes of Health under grants HL65425 and HL91017

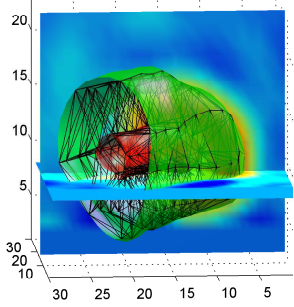


Fig. 1. Left ventricular mesh structure at the end diastole.

A. Motion estimation using a deformable mesh model

The proposed algorithm relies on a mesh representation of the left ventricle [17]. The motion estimation procedure presented in this paper has already been used and reported in [9], [10]. Here, we briefly recall the main steps of the procedure. Generation of the mesh structure is performed on pre-reconstructed images. Images used in this paper are reconstructed via filtered back-projection (FBP) but other reconstruction techniques might be used (e.g. expectation maximization [18] or others [19]). Filtered back-projection was performed without smoothing, spatial low-pass filtering is applied separately. Due to the noise in FBP reconstructions, generation of the initial mesh is applied on a time averaged version of the gated sequence. The time average image is further smoothed using a 3D Butterworth low-pass filter with order 4 and cutoff frequency 0.22 cycles per pixel. The resulting image is used to fit a left ventricular model using the surface model reported in [11]. This method is used to generate a set of nodes located on the heart endocardial and epicardial surfaces. Tetrahedral mesh elements are then obtained from the set of mesh nodes via Delaunay triangulation [20] (implemented using the QuickHull algorithm [21]). A total of around 170 nodes is defined including supporting nodes ensuring proper triangulation (i.e. avoiding flat tetrahedrons). An example of mesh structure generated using this procedure is shown on Fig. 1.

The initial mesh structure is then deformed to track the myocardium motion. Motion estimation is performed by finding the nodal displacement that minimizes the cost function J defined as:

$$J(\mathbf{D}^{(k,l)}) = w E_m(\mathbf{D}^{(k,l)}) + (1 - w) E_s(\mathbf{D}^{(k,l)}), \quad (1)$$

where $\mathbf{D}^{(k,l)}$ is the set of nodal displacement between frames k and l and w weights the cost function in terms of the matching criterion E_m and the smoothing constraint E_s . The matching error E_m , a modified version of the block matching

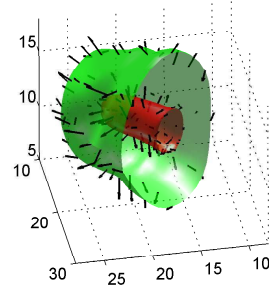


Fig. 2. Mesh at the end systole with motion field to the end diastolic frame displayed (black arrows).

method [22], is defined by:

$$E_m(\mathbf{D}^{(k,l)}) = \sum_{m=1}^M \int_{\mathcal{D}_m} \left(f^{(k)}(\mathbf{x}) - f^{(l)}(\mathbf{x} + \mathbf{d}^{(k,l)}(\mathbf{x})) \left(\frac{|\mathcal{D}_m^{(l)}|}{|\mathcal{D}_m^{(k)}|} \right) \right)^2 dx,$$

where $f^{(k)}(\mathbf{x})$ is the intensity of the reconstructed image at frame k and location \mathbf{x} , $\mathbf{d}^{(k,l)}(\mathbf{x})$ represents the displacement between frames k and l , $\mathcal{D}_m^{(k)}$ denotes the mesh element m at frame k and $|\mathcal{D}_m^{(k)}|$ represents its volume. The intensity matching process is rescaled by the volume in order to reflect the relation existing between myocardial contraction and image brightening (due to partial volume effect). Indeed, as shown in [7], intensity increases linearly as the myocardium contracts. More details on the evaluation of the matching error can be found in [17] and [23].

The smoothing constraint used in (1), is defined by:

$$E_s(\mathbf{D}^{(k,l)}) = \sum_{n=1}^N \left\| \mathbf{d}_n^{(k,l)} - \bar{\mathbf{d}}_n^{(k,l)} \right\|^2,$$

where $\mathbf{d}_n^{(k,l)}$ is the displacement of node n and $\bar{\mathbf{d}}_n^{(k,l)}$ is the average displacement of its neighboring nodes.

In practice, motion estimation is performed between successive frames and the time sequence is processed several times assuming $\mathbf{D}^{(K,K+1)} = \mathbf{D}^{(K,1)}$ where K is the total number of time frames. An example of motion field obtained using this technique is shown on Fig. 2.

B. Motion-compensated summation

In this section, we introduce the technique used to perform motion-compensated summation. Once the nodal displacement has been estimated, the image can be averaged over the time dimension so that the resulting static image contains counts from all frames. Using this approach, the gated sequence can be warped to any time frame k using:

$$\hat{f}^{(k)} = \sum_{l=1}^K f^{(l)}(\mathbf{x} + \mathbf{d}^{(k,l)}(\mathbf{x})) \left(\frac{|\mathcal{D}_m^{(l)}|}{|\mathcal{D}_m^{(k)}|} \right). \quad (2)$$

In (2), the motion $\mathbf{d}^{(k,l)}(\mathbf{x})$ is linearly interpolated from the nodal displacement estimated earlier. In addition, partial volume effect is accounted for as it is during motion estimation.

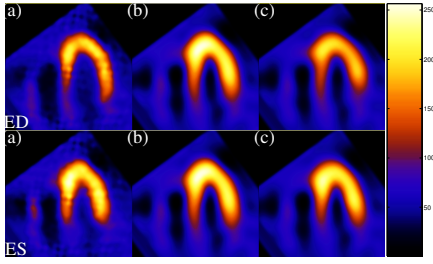


Fig. 3. Horizontal long-axis views at the end diastole (ED) and the end systole (ES) for (a) reconstruction of noiseless projections, (b) rigid summation and (c) proposed motion-compensated summation.

The summed image is further processed using a Butterworth low-pass filter with order 5 and cutoff frequency 0.22 cycles per pixel as reported in [24] in a clinical setup.

III. RESULTS

Here we present the results obtained using the proposed motion-compensated summation method. Simulations were performed using the NCAT phantom [25] and the SIMIND program [26] in order to simulate a gated SPECT acquisition. Poisson noise was then added at a level corresponding to half a million counts originated from the heart region. FBP was used for reconstruction, generating images with dimensions $64 \times 64 \times 64 \times 16$ (with pixel size 0.634 cm^3). The proposed method is compared to a rigid summation along the time dimension with no motion correction. The FBP reconstruction of noiseless projections is used as a reference for quantitative evaluation.

Visual comparison is shown on Fig. 3 between long-axis views of (a) reconstruction of noiseless projections (Ref), (b) rigid summation (Sum) and (c) proposed motion-compensated summation (MC). Note that the rigid and proposed summed images were processed with a low-pass Butterworth filter with order 5 and cutoff frequency 0.22 cycles per pixel. The images suggest that the proposed method achieves better noise reduction while avoiding motion blur. Rigid summation deforms the shape of the myocardium and therefore degrades visibility of the left ventricle structure. Besides, rigid summation exhibits excessive brightness especially near the apex, while the proposed method shows more fidelity to the reference image. Additionally, simple temporal summation yields a single image while the proposed method can be used to warp the sequence to an arbitrary gate. A similar analysis can be drawn from visualization of short-axis views on Fig. 4. To validate our method, it was applied on a clinical dataset containing FBP reconstructions of projections obtained from a healthy patient. Horizontal long axis views shown on Fig. 5 suggest that the proposed method efficiently avoids motion-blur compared to rigid summation. When warped to the end diastole, the proposed method results in a dimmer left ventricle which corresponds to the end diastolic form, where simple summation degrades the shape. Besides, the proposed method exhibits myocardium brightening, which is often clinically used to assess wall motion.

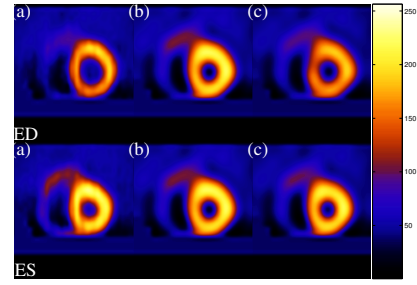


Fig. 4. Short-axis views at the end diastole (ED) and the end systole (ES) for (a) reconstruction of noiseless projections, (b) rigid summation and (c) proposed motion-compensated summation.

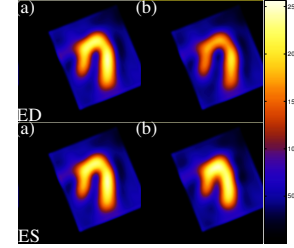


Fig. 5. Horizontal long-axis views for clinical data at the end diastole (ED) and the end systole (ES) for (a) rigid summation and (b) proposed motion-compensated summation.

To confirm visual improvement, we have performed noise reduction measurements over multiple noise realizations (50). The proposed method was evaluated when warping the gated sequence to another frame than the end diastole. Curves showing the peak signal-to-noise ratio (PSNR) for different warping frames are reported on Fig. 6. The proposed method outperforms rigid summation in most frames, especially at the end diastole (frame 1) and end systole (frame 8). In clinical environment, these frames are the most commonly used for assessment of a patient's condition (via ejection fraction measurements). Intermediate frames with index 4 and 12 represent frames where the heart is in its average stage and therefore simple average performs well. The curves shown on Fig. 6 were generated by applying temporal summation followed by a low-pass Butterworth filter. The optimal spatial cutoff frequency was used for filtering (i.e. $\omega_c = 0.22$ cycles per pixel). This optimal value was found by exhaustive search reported on Fig. 7. This figure shows that the proposed algorithm outperforms rigid summation for any spatial cutoff frequency i.e. for any trade-off between detail and smoothness of the image.

IV. CONCLUSION

We have developed a post-processing algorithm for motion-compensated summation of cardiac gated SPECT images. The proposed method relies on motion estimated using our previously introduced deformable mesh model. It is initially defined on the left ventricle and tracks the myocardium through the time sequence. The estimated motion is then utilized to perform temporal summation along the motion trajectory to correct for motion-blur. Quantitative

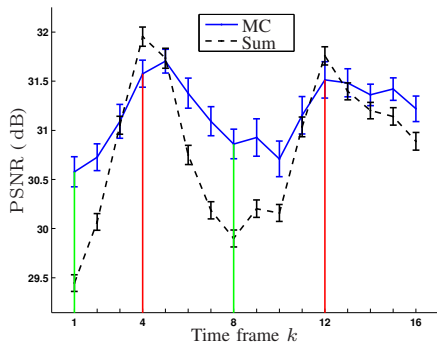


Fig. 6. PSNR as a function of the time frame k . Error bars show standard deviation over 50 noise realizations.

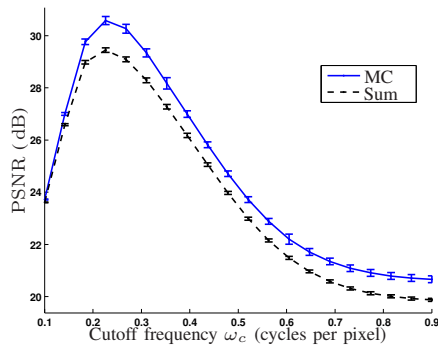


Fig. 7. PSNR as a function of ω_c cutoff frequency of the low-pass filter. Error bars show standard deviation over 50 noise realizations.

evaluation as well as processing of clinical data show that the proposed method offers better noise reduction than simple temporal averaging. Significant improvement has been shown in terms of noise reduction as well as in preserving the myocardium shape.

REFERENCES

- [1] C. L. Hansen, R. A. Goldstein, D. S. Berman, K. B. Churchwell, C. D. Cooke, J. R. Corbett, S. J. Cullom, S. T. Dahlberg, J. R. Galt, R. K. Garg, G. V. Heller, M. C. Hyun, L. L. Johnson, A. Mann, B. D. McCallister, R. Taillefer, R. P. Ward, J. J. Mahmarian, and Q. A. C. of the American Society of Nuclear Cardiology, "Myocardial perfusion and function single photon emission computed tomography," *Journal of Nuclear Cardiology*, vol. 13, no. 6, pp. e97–e120, November 2006.
- [2] A. I. Veress, G. T. Gullberg, and J. A. Weiss, "Measurement of strain in the left ventricle during diastole with cine-mri and deformable image registration," *Journal of Biomechanical Engineering*, vol. 127, no. 7, pp. 1195–1207, December 2005.
- [3] G. J. Klein, B. W. Reutter, and R. H. Huesman, "Non-rigid summing of gated pet via optical flow," *IEEE Transactions on Nuclear Science*, vol. 44, no. 4, pp. 1509–1512, August 1997.
- [4] B. K. Horn and B. G. Schunck, "Determining optical flow," *Artificial Intelligence*, vol. 17, pp. 185–203, 1981.
- [5] P. J. Slomka, H. Nishina, D. S. Berman, X. Kang, C. Akincioglu, J. D. Friedman, S. W. Hayes, U. E. Aladl, and G. Germano, "Motion-frozen display and quantification of myocardial perfusion," *Journal of Nuclear Medicine*, vol. 45, no. 7, pp. 1128–1134, July 2004.
- [6] Y. Suzuki, P. J. Slomka, A. Wolak, M. Ohba, S. Suzuki, L. D. Yang, G. Germano, and D. S. Berman, "Motion-frozen myocardial perfusion spect improves detection of coronary artery disease in obese patients," *Journal of Nuclear Medicine*, vol. 49, no. 7, pp. 1075–1079, July 2008.
- [7] J. R. Galt, E. V. Garcia, and W. L. Robbins, "Effects of myocardial wall thickness on spect quantification," *IEEE Transactions on Medical Imaging*, vol. 9, no. 2, pp. 144–150, June 1990.
- [8] J. G. Brankov, Y. Yang, and M. N. Wernick, "Spatiotemporal processing of gated cardiac spect images using deformable mesh modeling," *Medical Physics*, vol. 32, no. 9, pp. 2839–2849, September 2005.
- [9] T. Marin, M. N. Wernick, Y. Yang, and J. G. Brankov, "Motion-compensated spatio-temporal filtering of cardiac gated spect images," in *IEEE Nuclear Science Symposium Conference Record*, Dresden, Germany, October 2008, pp. 3734–3737.
- [10] —, "Motion-compensated post-processing of gated cardiac spect images using a deformable mesh model," in *SPIE Proceedings: Image Processing*, vol. 7259, no. 1, Lake Buena Vista, FL, USA, February 2009, p. 72592E.
- [11] T. L. Faber, C. D. Cooke, J. W. Peifer, R. I. Pettigrew, J. P. Vansant, J. R. Leyendecker, and E. V. Garcia, "Three-dimensional displays of left ventricular epicardial surface from standard cardiac spect perfusion quantification techniques," *Journal of Nuclear Medicine*, vol. 36, no. 4, pp. 697–703, April 1995.
- [12] M. A. King and T. R. Miller, "Use of a nonstationary temporal wiener filter in nuclear medicine," *European Journal of Nuclear Medicine*, vol. 10, no. 9-10, pp. 458–461, May 1985.
- [13] J. Peter, R. J. Jaszczak, B. F. Hutton, and H. M. Hudson, "Fully adaptive temporal regression smoothing in gated cardiac spect image reconstruction," *IEEE Transactions on Nuclear Science*, vol. 48, no. 1, pp. 16–23, February 2001.
- [14] D. S. Lalush and B. M. W. Tsui, "Block-iterative techniques for fast 4d reconstruction using a priori motion models in gated cardiac spect," *Physics in Medicine and Biology*, vol. 43, no. 4, pp. 875–886, April 1998.
- [15] B. A. Mair, D. R. Gilland, and J. Sun, "Estimation of images and nonrigid deformations in gated emission ct," *IEEE Transactions on Medical Imaging*, vol. 25, no. 9, pp. 1130–1144, September 2006.
- [16] E. Gravier, Y. Yang, M. A. King, and M. Jin, "Fully 4d motion-compensated reconstruction of cardiac spect images," *Physics in Medicine and Biology*, vol. 51, no. 18, pp. 4603–4619, September 2006.
- [17] J. G. Brankov, "Mesh modeling, reconstruction and spatio-temporal processing of medical images," Ph.D. dissertation, Illinois Institute of Technology, 3301 South Dearborn Street, Chicago, IL 60616, December 2002.
- [18] K. Lange and R. Carson, "Em reconstruction algorithms for emission and transmission tomography," *Journal of Computer Assisted Tomography*, vol. 8, no. 2, pp. 306–316, April 1984.
- [19] M. N. Wernick and J. N. Aarsvold, *Emission Tomography*, M. Wernick, Ed. Boston: Academic Press, 2004.
- [20] F. P. Preparata and M. I. Shamos, *Computational Geometry: An Introduction*. Berlin: Springer-Verlag, 1985.
- [21] C. B. Barber, D. P. Dobkin, and H. Huhdanpaa, "The quickhull algorithm for convex hulls," *ACM Transactions on Mathematical Software*, vol. 22, no. 4, pp. 469–483, December 1996.
- [22] V. E. Seferidis and M. Ghanbari, "General approach to block-matching motion estimation," *Optical Engineering*, vol. 32, no. 7, pp. 1464–1474, July 1993.
- [23] Y. Wang, O. Lee, and A. Vetro, "Use of two-dimensional deformable mesh structures for video coding. ii. the analysis problem and a region-based coder employing an active mesh representation," *IEEE Transactions on Circuits and Systems for Video Technology*, vol. 6, no. 6, pp. 647–659, December 1996.
- [24] P. H. Pretorius, M. A. King, H. C. Gifford, S. T. Dahlberg, F. Spencer, E. Simon, J. Rashkin, N. Botkin, W. Berndt, M. V. Narayanan, and J. A. Leppo, "Myocardial perfusion spect reconstruction: receiver operating characteristic comparison of cad detection accuracy of filtered backprojection reconstruction with all of the clinical imaging information available to readers and solely stress slices iteratively reconstructed with combined compensation," *Journal of Nuclear Cardiology*, vol. 12, no. 3, pp. 284–293, June 2005.
- [25] W. P. Segars, "Development and application of the new dynamic nurbs-based cardiac-torso (ncat) phantom," Ph.D. dissertation, University of North Carolina at Chapel Hill, 2001.
- [26] M. Ljungberg and S.-E. Strand, "A monte carlo program for the simulation of scintillation camera characteristics," *Computer methods and programs in biomedicine*, vol. 29, no. 4, pp. 257–272, August 1989.